J. Plasma Physics (2009), *vol.* 75, *part* 2, *pp.* 273–287. © 2008 Cambridge University Press
doi:10.1017/S0022377808007563 Printed in the United Kingdom

Minimum dissipative relaxed states applied to laboratory and space plasmas

B. DASGUPTA, DASTGEER SHAIKH, Q. HU and G. P. ZANK

Institute of Geophysics and Planetary Physics (IGPP), University of California, Riverside, CA 92521, USA
(dastgeer@ucr.edu)

(Received 17 April 2008 and in revised form 6 May 2008, first published online 8 October 2008)

Abstract. The usual theory of plasma relaxation, based on the selective decay of magnetic energy over the (global) magnetic helicity, predicts a force-free state for a plasma. Such a force-free state is inadequate to describe most realistic plasma systems occurring in laboratory and space plasmas as it produces a zero pressure gradient and cannot couple magnetic fields with flow. A different theory of relaxation has been proposed by many authors, based on a well-known principle of irreversible thermodynamics, the principle of minimum entropy production rate which is equivalent to the minimum dissipation rate of energy. We demonstrate the applicability of minimum dissipative relaxed states to various self-organized systems of magnetically confined plasma in the laboratory and in the astrophysical context. Such relaxed states are shown to produce a number of basic characteristics of laboratory plasma confinement systems and solar arcade structure.

1. Introduction and motivation

Self-organization is a natural process (Ortolani and Schnack 1993) in which a continuous system evolves toward some preferred states showing a form of order on long scales. Examples of such self-organization processes are ubiquitous in nature and in systems studied in the laboratory. These ordered states are very often remarkably robust, and their detailed structures are mostly independent of the way the system is prepared. The final state to which a system evolves generally depends on the boundary conditions and the inherent geometry of the particular device, but is relatively independent of the initial conditions. Self-organization in a plasma is generally called plasma relaxation. The seminal theory for plasma relaxation first proposed by Taylor (1974) yields a force-free state with zero pressure gradient. Taylor's theory was the first to explain the experimentally observed field reversal of the reversed field pinch (RFP).

Self-organized states with zero pressure gradient are often far from experimentally realizable scenarios. Any realistic magnetic configuration confining plasma must have a non-zero pressure gradient. Extensive numerical simulations (Zhu et al. 1995; Sato et al. 1996) have established the existence of self-organized states of plasma with finite pressure, i.e. these states are observed to be governed by the magnetohydrodynamic force balance equation. Numerical simulations (Dasgupta et al. 1995; Watanabe et al. 1997) and experiments (Ono et al. 1993) have established that

https://doi.org/10.1017/S0022377808007563 Published online by Cambridge University Press

counterhelicity merging of two spheromaks can produce a field-reversed configuration (FRC). The FRC has a zero toroidal magnetic field, and the plasma is confined entirely by the poloidal magnetic field. It has a finite pressure, non-zero perpendicular component of current and is more often characterized by a high value of plasma beta. The stability and long life categorize the FRC as a relaxed state, which is not obtainable from the Taylor model of relaxation. Since spheromaks are depicted as a Taylor state (Rosenbluth and Bussac 1979), formation of a FRC from the merging of two counterhelicity spheromaks is a unique process from the point of view of plasma relaxation, where a non-force-free state (hence non-Taylor state) emerges from the coalescence of two Taylor states. In an astrophysical context, particularly solar physics scenarios, a three-dimensional magnetohydrodynamics (MHD) simulation by Amari and Luciano (2000), among others, showed that, after the initial helicity drive, the final 'relaxed state is far from the ... linear force-free model that would be predicted by Taylor's conjecture' and they suggested the derivation of an alternative variational approach. Such physical processes call for an alternate model for plasma relaxation to broadly accommodate a large number of these observations.

In this context, an important work by Turner deserves special attention. Turner (1986) first showed that a relaxed magnetic field configuration can support/confine a plasma with a finite pressure gradient. Adopting a two-fluid approach, a model of magnetofluid relaxation is constructed for Hall MHD, under the assumptions of minimum energy (magnetic plus fluid) with the constraints of global magnetic helicity, hybrid helicity, axial magnetic flux and fluid vorticity. Euler–Lagrange equations resulting from such a variational approach show the coupling between the magnetic field and the fluid vorticity. The solutions for such coupled equations are shown to be achieved by the linear superposition of the eigen-vectors of the 'curl' operator (force-free states). These solutions yield magnetic field configurations which can confine plasma with a finite pressure gradient.

The principle of 'minimum rate of entropy production' formulated by Prigogine and others (Prigogine 1947) is believed to play a major role in many problems of irreversible thermodynamics. This principle states that, for any steady irreversible processes, the rate of entropy production is minimum. For most irreversible processes in nature, the minimum rate of entropy production is equivalent to the minimum rate of energy dissipation. A magnetized plasma is such a dissipative system and it is appropriate to expect that the principle of minimum dissipation rate of energy has a major role to play in a magnetically confined plasma. It is worth mentioning that Rayleigh (1873) first used the term 'principle of least dissipation of energy' in his works on the propagation of elastic waves in matter. Chandrasekhar and Woltjer (1958) considered a relaxed state of a plasma with minimum Ohmic dissipation with the constraint of constant magnetic energy and obtained an equation for the magnetic field involving a 'double curl' and remarked that the solution of such an equation is 'much wider' than the usual force-free solution.

Montgomery and Phillips (1988) first used the principle of minimum dissipation rate (MDR) of energy in an MHD problem to understand the steady profile of a RFP under the constraint of a constant rate of supply and dissipation of helicity with the boundary conditions for a conducting wall. Farengo et al. (1994, 1995, 2002) (see also Bouzat 2006) in a series of papers applied the principle of MDR to a variety of problems ranging from a flux-core spheromak to a tokamak.

https://doi.org/10.1017/S0022377808007563 Published online by Cambridge University Press

In this work, we present an alternative scenario for plasma relaxation which is based on the principle of minimum dissipation rate (MDR) of energy. This model gives us a non-force-free magnetic field, capable of supporting a finite pressure gradient. We demonstrate that this model can reproduce some of the basic characteristics of most of the plasma confining devices in the laboratory as well as the arcade structure of a solar magnetic field. A two-fluid generalization of this model for an open system couples magnetic field with flow—so this model is applicable to other astrophysical situations.

The plan of the paper is as follows. In Sec. 2, we present a single fluid MDR model for a closed system and briefly discuss its applications to some of the laboratory plasma confinement devices, such as the RFP, spheromak, tokamak and FRC. We present the result of a recent numerical simulation to justify our choice of the energy dissipation rate as an effective minimizer in our variation problem. In Sec. 3 we describe a generalized version of the MDR model for an open two-fluid system and its application to the solar arcade problem. We summarize a numerical extrapolation method for a non-force-free coronal magnetic field based on our MDR model. Section 4 concludes our paper.

2. Single-fluid MDR-based model

To obtain both the field reversal and a finite pressure gradient for the RFP, Dasgupta et al. (1998) considered the relaxation of a slightly resistive and turbulent plasma using the principle of MDR under the constraint of constant global helicity. With the global helicity K_M and the dissipation rate R defined as

$$K_M = \int_V \mathbf{A}\cdot\mathbf{B}\,dV, \quad R = \int_V \eta\mathbf{j}^2\,dV, \tag{2.1}$$

the variational principle $\delta(R-\Lambda K)$ leads to the following Euler–Lagrange equation:

$$\nabla\times\nabla\times\nabla\times\mathbf{B} = \Lambda\mathbf{B}. \tag{2.2}$$

Solutions of the above equation can be constructed as a superposition of the force-free equation using Chandrasekhar–Kendall (CK) eigenfunctions (Chandrasekhar and Kendall 1957),

$$B = \alpha_1 B_1 + \alpha_2 B_2 + \alpha_3 B_3, \tag{2.3}$$

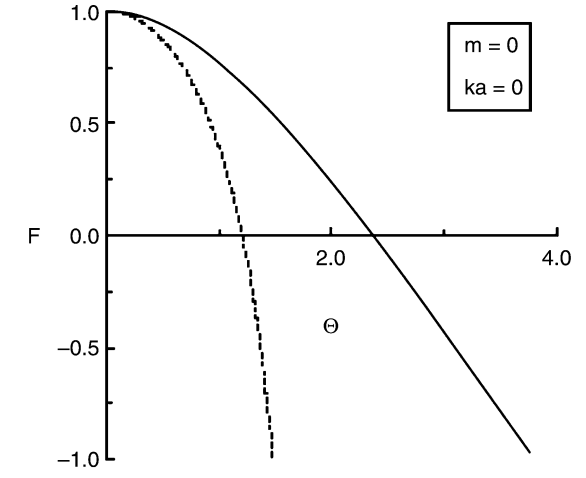
where $\alpha_1, \alpha_2, \alpha_3$ are constants, to be determined from the boundary conditions, and $\mathbf{B}_i$ are obtained from

$$\nabla\times\mathbf{B}_i = \lambda_i B_i \quad (i=1,2,3); \quad \lambda_i^3 = \Lambda. \tag{2.4}$$

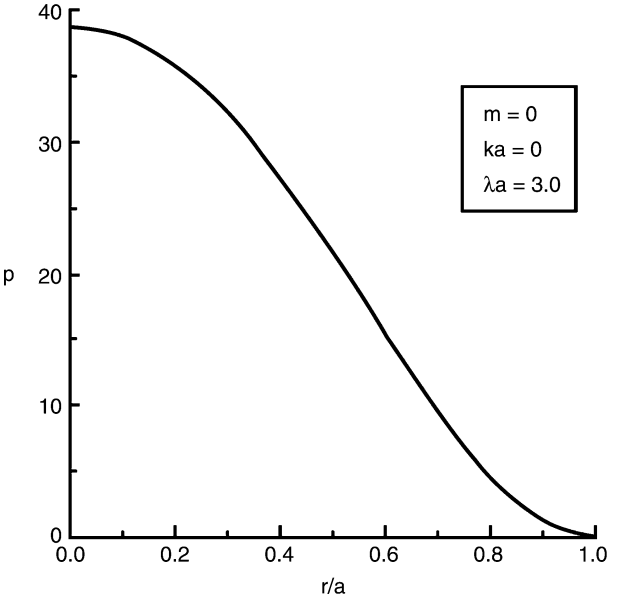
We have used the analytic continuation of CK eigenfunctions in the complex domain. However, one can easily ascertain that the resulting magnetic field B is real. Moreover, since the superposition of force-free fields with different eigenvalues λ_i is not a force-free field, the resultant magnetic field B is not force free, $\mathbf{J}\times\mathbf{B}\neq 0$. An explicit form of the solution in cylindrical geometry with the boundary conditions for an RFP (a perfectly conducting wall) has shown two remarkable features: (1) such a state can support a pressure gradient; and (2) field reversal is found in states that are not force free.

In Fig. 1 a plot of the field reversal parameter F against the pinch parameter Θ is shown. It is found that axial field reverses at a value $\Theta \simeq 2.2$; and Fig. 1(b) shows the pressure profile p(r) of the RFP obtained from our MDR model.

https://doi.org/10.1017/S0022377808007563 Published online by Cambridge University Press



(a)



(b)

Figure 1. (a) Plot of $F = B_z(a)/\langle B_z \rangle$ and $\Theta = B_\theta(a)/\langle B_z \rangle$ ($\langle \cdots \rangle$ is the volume average and a is the radial distance) showing the field reversal of the RFP obtained from the MDR model. The dotted curve represents the plot for the minimum energy state of Taylor. (b) Pressure profile of the RFP obtained from the MDR model. (Reprinted with permission from Dasgupta et al. (1998); Copyright (1998) by the American Physical Society.)

A success of this theory is its applicability in a tokamak configuration (Bhattacharya et al. 2000). In toroidal geometry, the CK eigenfunctions are hypergeometric functions in the large aspect ratio approximation. Equilibria can be constructed under the assumption that the total current J is equal to zero at the edge. The solution reproduces the q-profile, the toroidal magnetic field, the pressure

https://doi.org/10.1017/S0022377808007563 Published online by Cambridge University Press

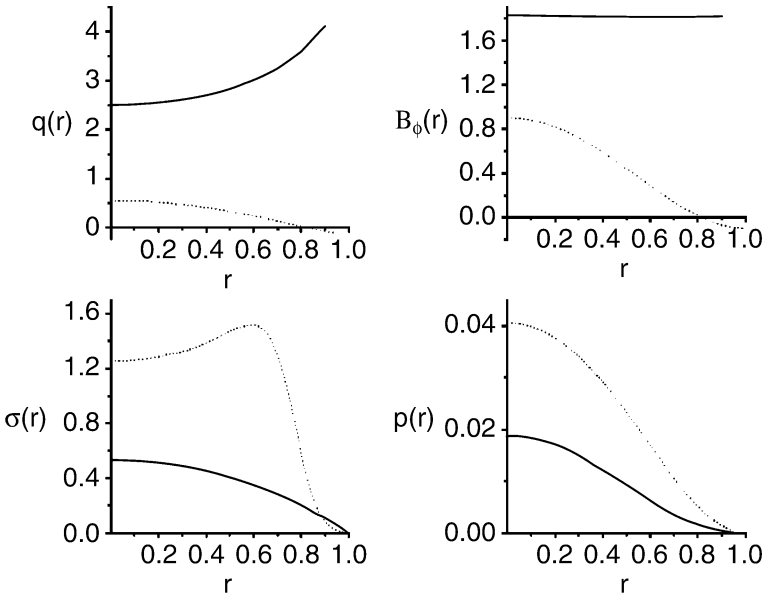


Figure 2. The q-profile, B_ϕ, σ and the pressure profile of (i) a tokamak discharge (continuous line); (ii) a RFP discharge (dotted line). (Reprinted with permission from Bhattacharya et al. (2000); Copyright (2000) by the American Institute of Physics.)

profile and $\sigma = \mathbf{J} \cdot \mathbf{B}/B^2$ for the tokamak which are very close to observed profiles (e.g., Fig. 2). The solutions allow for a tokamak, low-q discharge as well as RFP-like behavior with a change of eigenvalue which would essentially determine the number of volt-seconds associated with the discharge characterizing the relaxed state. The poloidal volt-seconds/toroidal flux associated with the discharge can be directly interpreted in terms of the parameter λr_0 (r_0 is the minor radius of the torus, $\lambda = \sqrt[3]{\Lambda}$) and can be shown to increase with λr_0. The MDR relaxed state can yield several kinds of solutions with distinct q-profiles. For low values of λr_0, the q-profile is monotonically increasing and hence the solutions resemble a tokamak-type discharge together with a nearly constant toroidal field; for larger values of λr_0, the toroidal field reverses at the edge signifying a RFP-type behavior, and for intermediate values, the relaxed states indicate an ultra low-q type of discharge exhibiting a q-profile with a pitch minimum and $0 < q < 1$. In Fig. 2, we plot the toroidal magnetic field $B_\phi, \sigma = \mathbf{J} \cdot \mathbf{J}/B^2, q$ and pressure profiles p(r) for different values of λr_0, for a fixed value of the aspect ratio equal to 4.0. The continuous line corresponds to $\lambda r_0 = 1.5$, and shows a monotonic increase with r, which is the essential feature of a tokamak discharge. For this case the toroidal magnetic field (B_ϕ) is essentially constant and the pressure profile has a peak at the center of the minor cross section of the torus and falls to zero at the edge. A non-constant behavior is shown by the σ profile. The dotted line corresponds to $\lambda r_0 = 3.0$. In this case the toroidal field reverses sign at the edge, which corresponds to a RFP-like discharge. The q-profile shows a similar behavior. The σ profile has a dip at $r = 0$ and exhibits a bump near the outer region. Such profiles have been experimentally observed in the ETA-BETA-II device (Antoni et al. 1983). For the values $\lambda r_0 = 2.5$ the q-profile shows a non-monotonic behavior as shown in Fig. 3.

https://doi.org/10.1017/S0022377808007563 Published online by Cambridge University Press

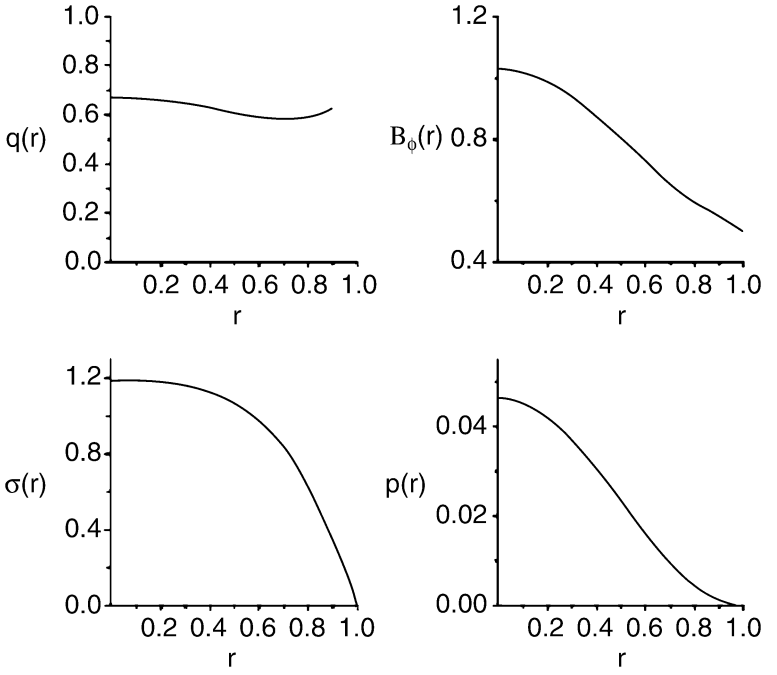


Figure 3. The q-profile, B_ϕ, σ and the pressure profile of a low-q discharge. (Reprinted with permission from Bhattacharya et al. (2000); Copyright (2000) by the American Institute of Physics.)

The toroidal magnetic field again peaks at the center and slowly decreases towards the edge, showing a paramagnetic behavior that is typical of a ultra low-q discharge (Yoshida et al. 1986). The pressure profile p(r) peaks at the center and goes to zero at the edge. Some of these results have been observed in the SINP tokamak (Lahiri et al. 1996) and were also reported earlier in REPUTE-1 (Yoshida et al. 1986) and in TORIUT-6 (Yamada et al. 1987).

This model has been utilized to obtain the spheromak configuration from the spherically symmetric solution under appropriate boundary conditions relevant to an insulating boundary at the edge (Dasgupta et al. 2002). These boundary conditions are consistent with the classical spheromak solution used by Rosenbluth and Bussac (1979). The most interesting part of this spheromak solution is the non-constant profile for $\mathbf{J} \cdot \mathbf{B}/B^2$ plotted against the normalized distance from the magnetic axis. This profile shows peaks outside the magnetic axis, and this feature is qualitatively closer to the experimentally observed profile reported by Hart et al. (1983).

The FRC is a compact toroidal confinement device (Tuszewski 1988) which is formed with primarily poloidal magnetic field and a zero or negligibly small toroidal magnetic field. The plasma beta of the FRC is one of the highest for any magnetically confined plasma. FRC can be considered as a relaxed state (Guo et al. 2005, 2006), but it is a distinctly non-Taylor state. The FRC configuration can be obtained for an externally driven dissipative system which relaxes with minimum dissipation. In Bhattacharya et al. (2001) we show that the Euler–Lagrange equations for relaxation under MDR with magnetic energy as the constraint represents

https://doi.org/10.1017/S0022377808007563 Published online by Cambridge University Press

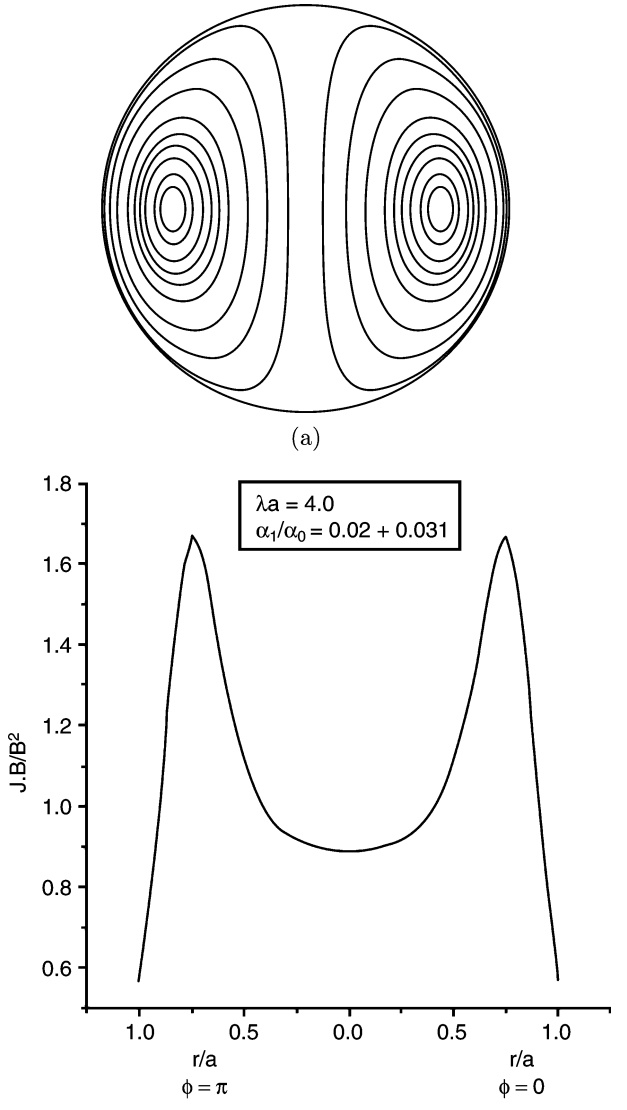


Figure 4. Spheromak configuration (a) and the non-constant $J_{\parallel}/B$ derived from our model based on MDR (b). (Reprinted with permission from Dasgupta et al. (2002); Copyright (2002) by the American Physical Society.)

an FRC configuration for one choice of eigenvalues. This solution is characterized by high beta, zero helicity and a completely null toroidal field, and it supports a non-constant pressure profile (non-force-free). Another choice of eigenvalue leads to a spheromak configuration. A generalization of this work incorporating flow (Bhattacharya et al. 2003) and taking magnetic and flow energies and cross helicities as constraints also produces the FRC. This state supports field-aligned flows with strong shears that may lead to stability and better confinement.

https://doi.org/10.1017/S0022377808007563 Published online by Cambridge University Press

2.1. Simulation results

To justify the use of the MDR principle in plasma relaxation and the choice of the total dissipation rate as a minimizer in the variational principle we performed a fully three-dimensional numerical simulation for a turbulent and slightly dissipative plasma using a fully compressible MHD code (Shaikh et al. 2007) with periodic boundary conditions. Fluctuations are Fourier expanded and nonlinear terms are evaluated in real space. Spectral methods provide an accurate representation in Fourier space. In our code there is very little numerical dissipation, and hence the ideal invariants are preserved. The selective decay processes (in addition to dissipation) depend critically on the cascade properties associated with the rugged MHD invariants that eventually govern the spectral transfer in the inertial range. This can be elucidated as follows (Biscamp 2003). The magnetic vector potential in three-dimensional MHD dominates over the magnetic field fluctuations at the smaller Fourier modes, which in turn leads to a domination of the magnetic helicity invariant over the magnetic energy. On the other hand, dissipation occurs predominantly at the higher Fourier modes which gives rise to a rapid damping of the energy dissipative quantity R. A heuristic argument for this process can be formulated in the following way. The decay rates of helicity K and dissipation rate $R = \int_V \eta j^2 dV$ in the dimensionless form, with the magnetic field Fourier decomposed as $\mathbf{B}(\mathbf{k}, t) = \Sigma_k \mathbf{b}_\mathbf{k} \exp(i\mathbf{k} \cdot \mathbf{r})$, can be expressed as

$$\frac{dK}{dt} = -\frac{2\eta}{S}\Sigma_k k {\mathbf{b}_\mathbf{k}}^2, \quad \frac{dR}{dt} = -\frac{2\eta^2}{S^2}\Sigma_k k^4 {\mathbf{b}_\mathbf{k}}^2, \tag{2.5}$$

where $S = \tau_R/\tau_A$ is the Lundquist number, and τ_R and τ_A are the resistive and Alfvén time scales, respectively. The Lundquist number in our simulations varies between 10^6 and 10^7. We find that, at scale lengths for which $k \approx S^{1/2}$, the decay rate of energy dissipation is $\sim O(1)$. However, at these scale lengths, helicity dissipation is only $\sim O(S^{-1/2}) \ll 1$. This physical scenario is consistent with our three-dimensional simulations. Figure 5 shows the time evolution of the global helicity K_M, total magnetic energy W_M and the total dissipation rate R. It is seen that global helicity remains approximately constant (decaying very slightly during the simulation time) while the magnetic energy decays faster than the global helicity, but the energy dissipation rate decays even faster than the magnetic energy. The results of the simulation show that the total dissipation rate can serve as a minimizer during a relaxation process.

3. MDR-based relaxation model for a two-fluid plasma with external drive

Recently, Bhattacharya and Janaki (2004) developed a theory of dissipative relaxed states in a two-fluid plasma with external drive. We describe the plasma (consisting of ions and electrons) by the two-fluid equations. The basic advantages of a two-fluid formalism over the single-fluid or MHD counterpart are: (i) in a two-fluid formalism, one can incorporate the coupling of plasma flow with the magnetic field in a natural way, and (ii) the two-fluid description, being more general than MHD, is expected to capture certain results that are otherwise unattainable from a single-fluid description. It should be mentioned that although we are invoking the principle of minimum dissipation rate of energy—instead of the principle of

https://doi.org/10.1017/S0022377808007563 Published online by Cambridge University Press

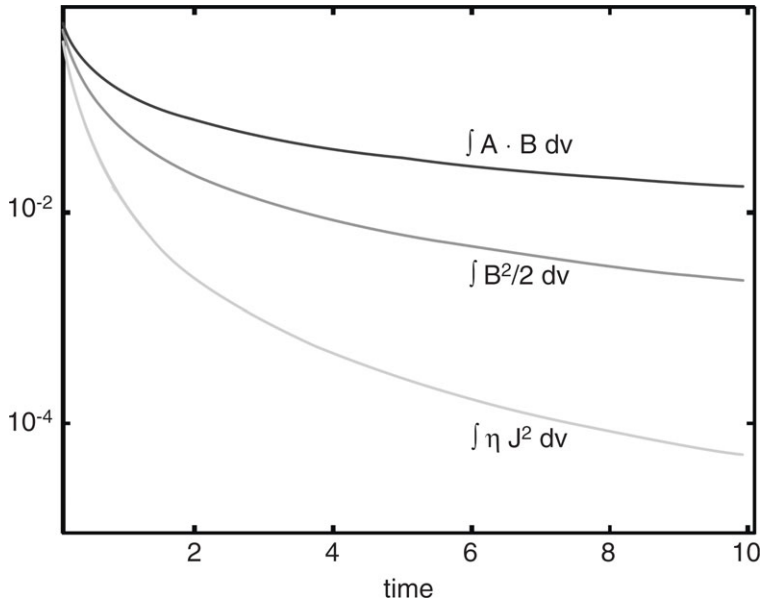


Figure 5. Time evolution of decay rates associated with the turbulent relaxation of the ideal MHD invariants, viz., global magnetic helicity $K_M = \int_V \mathbf{A} \cdot \mathbf{B}\, dV$, magnetic energy $W = \int_V B^2/2\, dV$ and the total dissipation $R = \int_V \eta J^2\, dV$, all shown on the same scale. (Reprinted with permission from Shaikh et al. (2008); Copyright (2008) by the American Institute of Physics.)

minimum energy—our approach is similar to the approach to plasma relaxation including Hall terms, as developed by Turner (1986).

In the two-fluid formalism the canonical momentum $\mathbf{P}_j$ and canonical vorticity $\mathbf{\Omega}_j$ for the jth species are defined respectively as

$$\mathbf{P}_j = m_j \mathbf{u}_j + \frac{q_j}{c}\mathbf{A}, \quad \mathbf{\Omega}_j = \nabla \times \mathbf{P}_j \quad (j = i, e). \tag{3.1}$$

A gauge invariant expression for the generalized helicity is introduced by defining

$$K_j = \int_V \mathbf{P}_j \cdot \mathbf{\Omega}_j\, d\tau - \int_V \mathbf{P}'_j \cdot \mathbf{\Omega}'_j\, dV, \tag{3.2}$$

which is a relative helicity with respect to the reference field having $\mathbf{P}'_j$ as the canonical momentum, and $\mathbf{P}_\alpha$ and $\mathbf{P}'_\alpha$ are different inside the volume of interest and the same outside. The gauge invariance condition holds:

$$(\mathbf{\Omega}_j - \mathbf{\Omega}'_j) \cdot \hat{n} = 0 \Rightarrow (\mathbf{B} - \mathbf{B}') \cdot \hat{n} = 0, \quad (\boldsymbol{\omega}_j - \boldsymbol{\omega}'_j) \cdot \hat{n} = 0 \quad (\boldsymbol{\omega}_j = \nabla \times \mathbf{u}_j), \tag{3.3}$$

under the condition that there is no flow-field coupling at the surface. The above equations then represent natural boundary conditions inherent to the problem.

The helicity balance equation for the generalized helicity, obtained from the balance equations for the generalized momentum and vorticity, consists of two terms: the helicity injection terms and the helicity dissipation term (containing resistivity and viscosity). The global helicity can be taken as a bounded function following Montgomery et al. (1988) and it is possible to form a variational problem

https://doi.org/10.1017/S0022377808007563 Published online by Cambridge University Press

with the helicity dissipation rates as constraints. Thus,

$$\frac{dK_\alpha}{dt} = -\oint [G_\alpha - \mathbf{P}_\alpha \cdot \mathbf{u}_\alpha]\boldsymbol{\Omega}'_\alpha \cdot \hat{n}\, da - \oint (\mathbf{P}_\alpha \cdot \boldsymbol{\Omega}_\alpha)\mathbf{u}_\alpha \cdot \hat{n}\, da$$

$$- \oint \left(\frac{\partial \mathbf{P}'_\alpha}{\partial t} \times \mathbf{P}'_\alpha\right) \cdot \hat{n}\, da - \eta'_\alpha \oint [\{\nabla \times \mathbf{B} + L_\alpha \boldsymbol{\omega}_\alpha)\} \times \mathbf{P}_\alpha] \cdot \hat{n}\, da$$

$$- 2\eta'_\alpha \int [\nabla \times (\mathbf{B} + L_\alpha \boldsymbol{\omega}_\alpha)] \cdot \boldsymbol{\Omega}_\alpha\, d\tau \tag{3.4}$$

with

$$G_\alpha = \left[q_\alpha \phi + \frac{h_\alpha}{n_\alpha} - \frac{m_\alpha u_\alpha^2}{2}\right], \quad \eta'_\alpha = \frac{q_\alpha \eta c}{4\pi}$$

$$L_\alpha = \frac{4\pi}{q_\alpha c n_\alpha}\frac{\mu_\alpha}{\eta} \equiv \text{Prandtl number.} \tag{3.5}$$

The minimization integral is then obtained as

$$\mathscr{I} = \int \left[(\nabla \times \mathbf{B}) \cdot (\nabla \times \mathbf{B}) + \frac{4\pi n q L_i}{c}\boldsymbol{\omega}_i \cdot \boldsymbol{\omega}_i\right] d\tau$$

$$+ \lambda_i \int [\nabla \times (\mathbf{B} + L_i \boldsymbol{\omega}_i)] \cdot \boldsymbol{\Omega}_i\, d\tau - \lambda_e \int (\nabla \times \mathbf{B}) \cdot \boldsymbol{\Omega}_e\, d\tau \tag{3.6}$$

where $L_i = 4\pi\mu_i/ecn_i\eta$ is the magnetic Prandtl number for ions, μ_i is the ion viscosity and η is the resistivity. We have assumed the electron mass $m_e \to 0$. The first two terms in the above integral represent the ohmic and viscous dissipation rates while the second two integrals represent the ion and electron generalized helicity dissipation rates, respectively. λ_i and λ_e are the corresponding Lagrange undetermined multipliers.The Euler–Lagrange equations are written as

$$\nabla \times \nabla \times \mathbf{B} + \frac{(\lambda_i + \lambda_e)q}{c}\nabla \times \mathbf{B} + \frac{\lambda_i}{2}\left(\frac{qL_i}{c} + m_i\right)(\nabla\times)\boldsymbol{\omega}_i = \nabla\psi, \tag{3.7}$$

$$\nabla \times \nabla \times \boldsymbol{\omega}_i + \frac{2\pi n q}{m_i \lambda_i c}\nabla \times \boldsymbol{\omega}_i + \frac{1}{2m_i L_i}\left(\frac{qL_i}{c} + m_i\right)(\nabla\times)^2\mathbf{B} = \nabla\chi, \tag{3.8}$$

where ψ and χ are arbitrary gauge functions, with $\nabla^2\psi = \nabla^\chi = 0$. Following Turner (1986) we can write the exact solution of the coupled equations (3.7) and (3.8) as a linear superposition of two CK eigenfunctions, which are the solutions of $\nabla \times \mathbf{Y}_k = \lambda_k \mathbf{Y}_k$, i.e.

$$\mathbf{B} = \mathbf{Y}_1 + \alpha\mathbf{Y}_2 \quad \omega_i = \mathbf{Y}_1 + \beta\mathbf{Y}_2, \tag{3.9}$$

and α and β are constants and quantify the non-force-free part, to be obtained from some boundary conditions.

3.1. Application to solar arcade problem

One of the important features of this formalism is the presence of a non-trivial flow and the coupling between the magnetic field and the flow. The solutions of the corresponding Euler–Lagrange equation highlight the role of non-zero plasma flow in securing a steady MDR relaxed state for an open and externally driven system. This model has been very successful in describing the arcade structures

https://doi.org/10.1017/S0022377808007563 Published online by Cambridge University Press

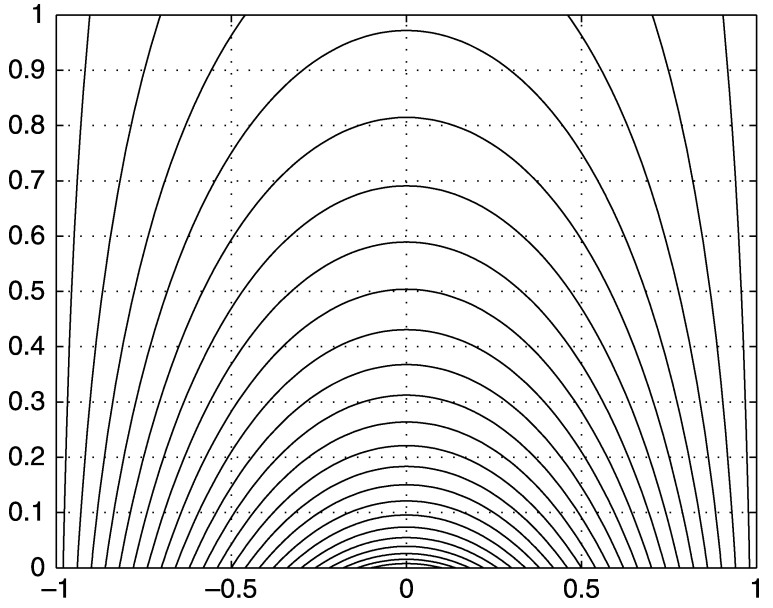


Figure 6. Flow lines in the x–z plane for $\gamma = 1.5$. (from Bhattacharya et al., (2007); reprinted with kind permission from Springer Science and Business Media. Copyright (2007) by the Springer Science and Business Media.)

observed in Solar corona (from Bhattacharya et al. (2007); reprinted with kind permission from Springer Science and Business Media. Copyright (2007) by the Springer Science and Business Media.). To model solar arcade-type magnetic fields, we make some simplified assumptions and consider a two-dimensional magnetic field in the x–z plane with the x-direction lying on the photosphere surface and z being in the vertical direction. With appropriate boundary conditions and after some lengthy algebra, the solutions for the components of the magnetic fields are obtained as

$$B_x = \sqrt{\gamma^2-1}\left[2\cos\gamma x - \frac{2\cos\gamma}{\cos\sqrt{\gamma^2-1}}\cos(x\sqrt{\gamma^2-1})\right]e^{-z\sqrt{\gamma^2-1}},$$

$$B_y = 0, \tag{3.10}$$

$$B_z = -\left[2\gamma\sin\gamma x - \frac{2\sqrt{\gamma^2-1}\cos\gamma}{\sin\sqrt{\gamma^2-1}}\sin(x\sqrt{\gamma^2-1})\right]e^{-z\sqrt{\gamma^2-1}},$$

with $\gamma = \sqrt{(k^2+\lambda^2)/\lambda^2}$ (λ is the eigenvalue and k is the wave number associated with the solution). The same procedures can be adopted for the flow pattern. In Fig. 7 the magnetic field lines in the x–z plane are plotted for the value of the parameter $\gamma = 3.36$. The arcade structures are obtained by solving the field line equations $dz/dx = B_z/B_x$. It is interesting to note that the arcade structure changes with the change of the single parameter γ. Figure 6 plots the flow lines for $\gamma = 1.5$. In cylindrical geometry the solutions of (3.7) can be written in terms of a superposition of Bessel functions. Such solutions yield three-dimensional flux ropes, which are plotted in Fig. 8.

https://doi.org/10.1017/S0022377808007563 Published online by Cambridge University Press

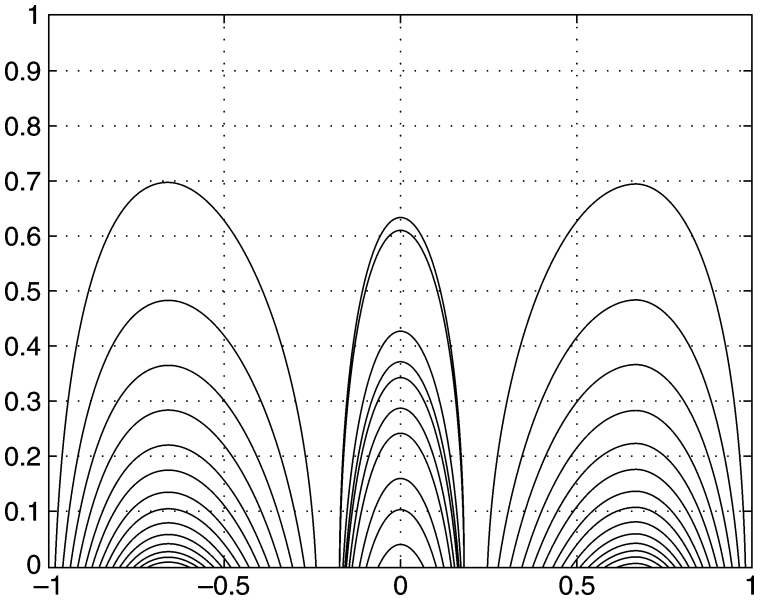


Figure 7. Magnetic field lines in the x–z plane corresponding to a triple arcade structure for $\gamma = 3.36$ (from Bhattacharya et al., (2007); reprinted with kind permission from Springer Science and Business Media. Copyright (2007) by the Springer Science and Business Media.)

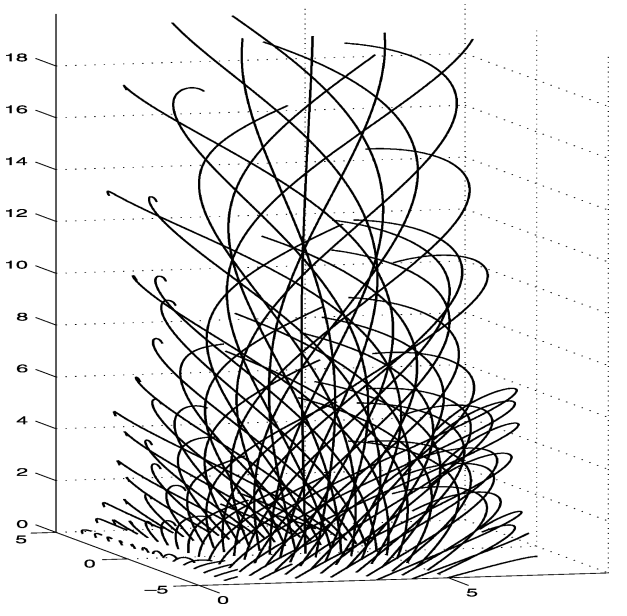


Figure 8. Plot of a three-dimensional flux rope obtained from the solution (3.7).

3.2. Non-force-free coronal magnetic field extrapolation based on MDR

An outstanding problem in solar physics is to derive the coronal magnetic field structure from measured photospheric and/or chromospheric magnetograms. A new approach to deriving three-dimensional non-force-free coronal magnetic field

https://doi.org/10.1017/S0022377808007563 Published online by Cambridge University Press

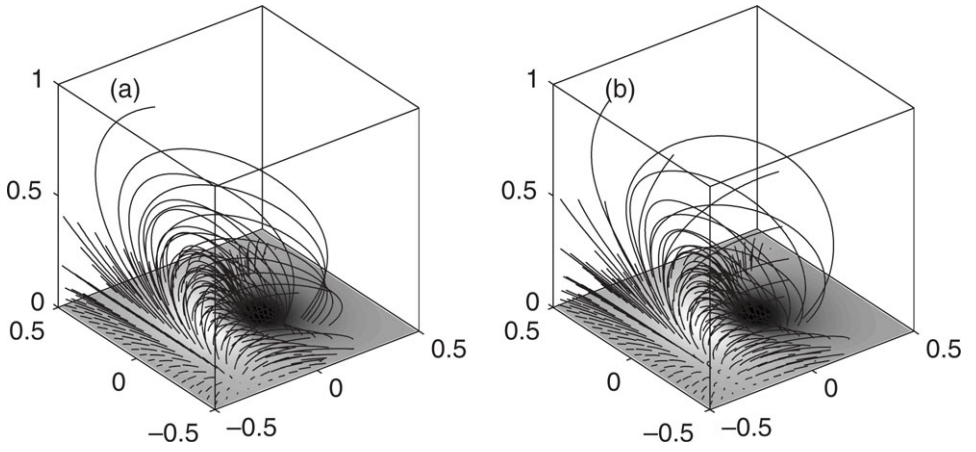


Figure 9. A three-dimensional view of magnetic field lines in a box simulating the typical extrapolation domain. (a) Exact solution; (b) numerical extrapolation result. The bottom image at height 0 shows the normal field component distribution with gray scale indicating strongly negative (black) to positive (white) field. The great resemblance between the exact and the numerical solutions justifies the feasibility and high performance of this method (Reprinted with permission from Hu et el. (2007); Copyright (2007) by the American Institute of Physics.)

configurations from vector magnetograms, based on the MDR principle, has recently been developed (Hu et al. 2007). In contrast to the principle of minimum energy, which yields a linear force-free magnetic field, the MDR gives a more general non-force-free magnetic field with flow. The full MDR-based approach requires two layers of vector magnetic field measurements. Its exact solution can be expressed as the superposition of two linear force-free fields with distinct λ parameters, and one potential field. The final solution is thus decomposed into three linear force-free extrapolations, with bottom boundary conditions derived from the measured vector magnetograms, at both photospheric and chromospheric levels. The semi-analytic test case shown in Fig. 9 illustrates the feasibility and the high performance of this method. This extrapolation is easy to implement and much faster than most other nonlinear force-free methods (Hu and Dasgupta 2007). It also takes full advantage of multiple-layer solar magnetic field measurements, thus giving a more realistic result.

4. Conclusion

We have demonstrated that a relaxation model based on the minimum dissipation of energy can successfully explain some of the salient observations both in laboratory and space plasmas. A MDR-based model in its simpler form is capable of yielding the basic characteristics of most of the laboratory plasma confinement devices, and a generalization of this model for two fluids with external drive can couple the magnetic field and flow and predict solar arcade structures. The above findings definitely point out that the MDR relaxed states applied to astrophysical plasmas are a worthy case for further investigations. In future we plan to apply this model to investigate the magnetic field structure in the sun with the aim of understanding coronal mass ejection.

https://doi.org/10.1017/S0022377808007563 Published online by Cambridge University Press

Acknowledgements

We gratefully acknowledge partial support from NASA LWS grant NNX07A073G, NASA grants NNX08AH46G, NNG04GF83G, NNG05GH38G and NNG05GM62G, a Cluster University of Delaware subcontract BART372159/SG, and NSF grants ATM0317509 and ATM0428880.

References

Amari, T. and Luciani, J. F. 2000 Helicity redistribution during relaxation of astrophysical plasmas. *Phys. Rev. Lett.* **84**, 1196–1199.

Antoni, V., Martini, S., Ortolini S. and Paccagnella, R. 1983 *Workshop on Mirror-based and Field-reversed Approaches to Magnetic Fusion, International School of Plasma Physics, Varenna, Italy*, p. 107.

Bhattacharya, R., Janaki, M. S. and Dasgupta, B. 2000 Tokamak, reversed field pinch and intermediate structures as minimum-dissipative relaxed states. *Phys. Plasmas* **7**, 4801–4804.

Bhattacharya, R., Janaki, M. S. and Dasgupta, B. 2001 Field-reversed configuration (FRC) as a minimum-dissipative relaxed state. *Phys. Lett.* A **291A**, 291–295.

Bhattacharya, R., Janaki, M. S. and Dasgupta, B. 2003 Relaxation phenomenon in the field reversed configuration. *Plasma Phys. Control. Fusion* **45**, 63–70.

Bhattacharya, R. and Janaki, M. S. 2004 Dissipative relaxed states in two-fluid plasma with external drive. *Phys. Plasmas* **11**, 5615–5619.

Bhattacharya, R., Janaki, M. S., Dasgupta, B. and Zank, G. P. 2007 Solar arcades as possible minimum dissipative relaxed states. *Solar Phys.* **240**, 63–76.

Biskamp, D. 2003 *Magnetohydrodynamic Turbulence*. Cambridge University Press.

Bouzat, S. and Farengo, R. 2006 Analytical solutions for minimum dissipation states: flux core spheromak sustained by helicity injection. *J. Plasma Phys.* **72**, 443–456.

Chandrasekhar, S. and Kendall, P. C. 1957 On force-free magnetic fields. *Astrophys. J.* **126**, 457–459.

Chandrasekhar, S. and Woltjer, L. 1958 On force-free magnetic fields. *Proc. Natl. Acad. Sci. USA* **44**, 285–289.

Dasgupta, B., Dasgupta, P., Janaki, M. S., Watanabe, T. and Sato, T. 1998 Relaxed states of a magnetized plasma with minimum dissipation. *Phys. Rev. Lett.* **81**, 3144–3147.

Dasgupta, B., Janaki, M. S., Bhattacharya, R., Dasgupta, P., Watanabe, T. and Sato, T. 2002 Spheromak as a relaxed state with minimum dissipation. *Phys. Rev.* E **E65**, 046405 1–6.

Dasgupta, B., Sato, T., Hayashi, T., Watanabe, K. and Watanabe, T.-H. 1995 Formation of a field reversed configuration by coalescence of Spheromaks. *Trans. Fusion Technol.* **27**, 374–377.

Farengo, R. and Caputi, K. I. 2002 Relaxed, minimum dissipation states, for a flux core spheromak sustained by helicity injection. *Plasma Phys. Control. Fusion* **44**, 1707–1722.

Farengo, R. and Sobehart, J. R. 1994 Minimum ohmic dissipation and DC helicity injection in tokamak-like plasmas. *Plasma Phys. Control. Fusion* **36**, 1691–1700.

Farengo, R. and Sobehart, J. R. 1995 Determination of minimum-dissipation states with self-consistent resistivity in magnetized plasma. *Phys. Rev.* E **52**, 2102–2105.

Guo, H. Y., Hoffman, A. L., Steinhauer, L. C. and Miller, K. E. 2005 Observations of improved stability and confinement in a high-β self-organized spherical-torus-like field-reversed configuration. *Phys. Rev. Lett.* **95**, 175001, 1–4.

Guo, H. Y., Hoffman, A. L., Steinhauer, L. C., Miller, K. E. and Milroy, R. D. 2006 Evidence of relaxation and spontaneous transition to a high-confinement state in high-β steady-state plasmas sustained by rotating magnetic fields. *Phys. Rev. Lett.* **97**, 235002, 1–4.

Hart, G. W., Chin-Fatt, C., deSilva, A. W., Goldenbaum, G. C., Hess, R. and Shaw, R. S. 1983 Finite-pressure-gradient influences on ideal spheromak equilibrium. *Phys. Rev. Lett.* **51**, 1558–1561.

https://doi.org/10.1017/S0022377808007563 Published online by Cambridge University Press

Hu, Q. and Dasgupta, B. 2008 An improved approach to non-force-free coronal magnetic field extrapolation. *Sol. Phys.* **247**, 87–101.

Hu, Q., Dasgupta, B. and Choudhary, D. P. 2007 Application of the principle of minimum dissipation rate to solar coronal magnetic field extrapolation. In *Proc. 6th Annual International Astrophysics Conference: Turbulence and Nonlinear Processes in Astrophysical Plasmas, 16–22 March, Hawaii (AIP Conf. Proc., 932, American Institute of Physics*, ed. D. Shaikh and G. P. Zank), pp. 376–381.

Lahiri, S., Iyenger, A. N., Mukhopadhyay, S. and Pal, R. 1996 Accessibility of very low q_a (VLQ) and ultra-low q_a (ULQ) discharges in SINP tokamak. *Nucl. Fusion* **36**, 254–257.

Montgomery, D. and Phillips, L. 1988 Minimum dissipation rates in magnetohydrodynamics. *Phys. Rev.* A **38**, 2953–2964.

Ono, Y., Morita, A., Katsurai and Yamada, M. 1993 Experimental investigation of three-dimensional magnetic reconnection by use of two colliding spheromaks. *Phys. Fluids* B **B5**, 3691–3701.

Ortolani, S. and Schnack, D. D. 1993 *Magnetohydrodynamics of Plasma Relaxation*. Singapore: World Scientific.

Prigogine, I. 1946 *Etude Thermodynamique des Phénomènes Irreversibles*. Liège: Editions Desoer.

Rayleigh 1873 *Proc. Math Soc. London* **363**, 357.

Rosenbluth, M. N. and Bussac, M. N. 1979 MHD stability of spheromak. *Nucl. Fusion* **19**, 489–498.

Sato, T. and Complexity Simulation Group 1996 Complexity in plasma: from self-organization to geodynamo. *Phys. Plasmas.* **3**, 2135–2142.

Shaikh, D., Dasgupta, B., Zank, G. P. and Hu, Q. 2008 Theory and simulations of principle of minimum dissipation rate. *Phys. Plasmas.* **15**, 012306 1–5.

Taylor, J. B. 1974 Relaxation of toroidal plasma and generation of reverse magnetic fields. *Phys. Rev. Lett.* **33**, 1139–1141.

Turner, L. 1986 Hall effects on magnetic relaxation. *IEEE Trans. Plasma Sci.* **14**, 849–857.

Tuszewski, M. 1988 Field reversed configurations. *Nucl. Fusion* **28**, 2033–2092.

Watanabe, T.-H., Sato, T. and Hayashi, T. 1997 Magnetohydrodynamic simulation on co- and counter-helicity merging of spheromaks and driven magnetic reconnection. *Phys. Plasmas* **4**, 1297–1307.

Yamada, H., Kusano, K., Kamada, Y., Utsumi, H., Yoshida, Z. and Inoue, N. 1987 *Nucl. Fusion* **27**, 1169.

Yoshida, Z., Ishida, S., Hattori, K., Murakami Y., Morikawa, J., Nehei, N. and Inoue, N. 1986 Remarks on relaxation phenomenon in toroidal discharge. *J. Phys. Soc. Japan* **55**, 450–453.

Zhu, S., Horiuchi, R. and Sato, T. 1995 Non-Taylor magnetohydrodynamic self-organization. *Phys. Rev.* E **51**, 6047–6056.

https://doi.org/10.1017/S0022377808007563 Published online by Cambridge University Press